Pergamon

Chemical Engineering Science, Vol. 51, No. 3, pp. 353–363, 1996

0009–2509/96 $15.00 + 0.00

0009–2509(95)00236–7

THE INFLUENCE OF COALESCENCE ON DROPLET TRANSFER IN VERTICAL ANNULAR FLOW

ALFREDO SOLDATI† and PAOLO ANDREUSSI
Dipartimento di Scienze e Tecnologie Chimiche, Facoltà di Ingegneria, Università degli Studi di Udine, Via del Cotonificio 108, 33100 Udine, Italy

(*First received* 19 *November* 1994; *accepted in revised form* 30 *June* 1995)

Abstract—In vertical annular flow, the motion of droplets in the gas core is dominated either by a diffusion mechanism, when the droplet size is small, or by inertial effects when droplets are large. These two mechanisms have to be considered when predicting deposition rates. Furthermore, since droplet–droplet interactions influence droplet motion, a deposition model should also account for collisions and coalescence among droplets. After reviewing the available deposition models, the effect of coalescence on droplet motion is theoretically analyzed. The results demonstrate that coalescence extends droplets residence time in the gas core thus decreasing the deposition coefficient. On the basis of these results, a new deposition model which accounts for the two deposition mechanisms and includes the effect of coalescence is proposed and compared against existing experimental data.

1. INTRODUCTION

In annular gas–liquid flow, part of the liquid flows as a thin film at the pipe wall and part as droplets entrained in the gas core. Droplets are continuously generated at the gas–liquid interface and deposit back onto the wall layer. The relative magnitude of atomization and deposition rates determines the fraction of entrained liquid, which is often the critical parameter in modelling annular flow systems.

The deposition rate, R_D, is usually modelled by the turbulent transport equation (Cousins and Hewitt, 1968):

$$R_D = k C_E \tag{1}$$

where C_E is the droplet concentration in the gas core and k is the deposition coefficient. Andreussi and Azzopardi (1983) found that two different mechanisms control droplet transfer: smaller droplets, prevailing at large gas velocities, deposit after a random walk through the gas core determined by the interactions with gas-phase turbulence; larger droplets, typically produced at lower gas velocities, move through the gas core on a free flight, affected very little by turbulent eddies.

The analysis of the deposition phenomenon is complicated by a strong effect of droplet concentration on the deposition coefficient (Namie and Ueda, 1972; Andreussi, 1983; Leman *et al.*, 1985; Schadel *et al.*, 1990). On the basis of a similar effect of droplet concentration on droplet size detected by Azzopardi *et al.* (1980), Andreussi (1983) suggested that the dependence of the deposition coefficient on droplet concentration could be attributed to coalescence.

The objective of this work is to develop a physically based model of droplet deposition in annular flow capable of considering the contribution of the two deposition mechanisms and the effect of coalescence. The starting point is the work by Andreussi (1983), who presented a simple correlation for the diffusion deposition coefficient which considered the effect of droplet concentration. In the present paper, the attention is focused on drops which follow an inertially dominated motion. The influence of droplet–droplet interactions on the motion of such drops is examined theoretically. Then, a model for the deposition coefficient is set up and compared with experimental measurements.

Droplets entrained in the gas core may undergo two different types of interactions. A large, accelerating drop moves through the gas core slower than the gas and slower than smaller entrained droplets. Such a drop may interact with smaller droplets in a sweeping action, thus gaining axial momentum (axial interaction). A drop may also interact with other drops which move at about the same axial velocity but along different chords in the cross section (lateral interaction). This may be the case for small droplets fully entrained by the gas, which move at about the same axial velocity and are subject to lateral displacements.

In the first part of this work, this phenomenological representation of droplet–droplet interactions has been investigated analytically. In the following part, considering the theoretical results obtained, a physically based model of droplet deposition has been assessed against experimental data.

2. DROPLET DEPOSITION IN DILUTE SYSTEMS

2.1. *Deposition by diffusion*

The motion of a particle or a droplet in a turbulent flow field mainly depends on the characteristic relaxation time of the droplet (τ_d) compared to the characteristic time scale of the fluid (τ_f). The characteristic

†Corresponding author. Email: alfredo@euterpe.dstc.uniud.it.

relaxation time measures droplet responsiveness to a change in fluid velocity, while the fluid characteristic time is proportional to the turnover time of the turbulent eddies and it supplies a measure of the time available for eddy–particle interaction. For a liquid droplet entrained in a turbulent gas stream, assuming only the Stokes drag acting on the droplet, the ratio between the two characteristic times is the general definition of the Stokes number:

$$St = \frac{\tau_d}{\tau_f} = \left(\frac{\rho_l d^2}{18\mu_f}\right) \Big/ \left(\frac{l_l}{\sqrt{\overline{u'^2}}}\right) \tag{2}$$

where ρ_d and μ_f are, the droplet density and the dynamic viscosity of the gas, respectively, d is the droplet diameter, l_l is the Lagrangian microscale of turbulence and $\overline{u'^2}$ is the mean square of turbulent velocity fluctuations. A small droplet is characterized by a relatively small value of the Stokes number and is quickly entrained by turbulent eddies; its trajectory is closely dependent on turbulent velocity fluctuations and its velocity relative to the fluid one is negligible.

McCoy and Hanratty (1977) suggested that when interactions with turbulent eddies control droplet deposition, the diffusion deposition coefficient, k_D, made dimensionless with respect to the gas friction velocity, u^*, defined as

$$u^* = \sqrt{\tau_i/\rho_g} \tag{3}$$

where τ_i is the shear stress at the gas–liquid interface, should depend on the Stokes number only. For $St > 20$, which, usually, is the case in gas–liquid annular flow, McCoy and Hanratty (1977) proposed the following correlation:

$$\frac{k_D}{u^*} = \widetilde{k_D} = 0.17. \tag{4}$$

A more careful analysis of the phenomenon of droplet deposition by diffusion has recently led Lee *et al.* (1989) to conclude that deposition is, in this case, the result of two distinct phenomena in series: diffusion through the gas core and free flight through the viscous boundary layer to pipe-wall. The deposition coefficient by diffusion was then expressed as:

$$\frac{1}{\widetilde{k_D}} = \frac{1}{0.36\sqrt{\dfrac{\tau_{lf}/\tau_d}{0.7 + \tau_{lf}/\tau_d}}} + \frac{1}{0.25\,\varepsilon_d/\varepsilon_f} \tag{5}$$

where ε_d is the particle diffusivity, ε_f the fluid diffusivity, τ_{lf} is the Lagrangian time scale of the flow field. Using this expression, the maximum value attained by $\widetilde{k_D}$ is 0.15.

The experimental measurements of the rate of deposition performed by Andreussi (1983) under conditions where the diffusion mechanism is expected to be controlling, suggest that the maximum value of $\widetilde{k_D}$ for a dilute dispersion is 0.115. Leman *et al.* (1985) found a maximum value of $\widetilde{k_D}$ equal to 0.15. These measurements of k_D and the correlations given above are relative to dilute systems. As reported in the Introduction, a strong effect of droplet concentration has been noticed, among others, by Andreussi (1983) who correlated data relative to mean gas velocities above 40 m s^{-1} with the empirical equation:

$$\widetilde{k_D} = \frac{0.115}{1 + 2.3\,C_E/\rho_g} \tag{6}$$

which accounts explicitly for the dependence on droplet concentration.

2.2. *Deposition by impaction*

Droplet deposition after a free flight, by impaction, can be analyzed through the solution of the equation of motion of a droplet in a gas stream. In the present case, since the density of droplets is much larger than the density of the surrounding fluid, the droplet added mass, the Basset history term, and the hydrostatic force acting on the droplet can be neglected. About the lift force, usual corrections for turbulent flows prescribe the use of a time averaged velocity gradient. However, the existing uncertainties connected to such approach (Lee *et al.*, 1989) and experimental observations by Young and Hanratty (1991), highlight the unimportance of this effect outside the viscous region, and suggest the lift force to be negligible for the treated case. Finally, the droplet is small enough to neglect internal circulation. Therefore, the vectorial momentum equation for a spherical, rigid particle of diameter d and density ρ_l in a fluid of density ρ_g, can be expressed as:

$$m_d \frac{\mathrm{d}\mathbf{u}_d}{\mathrm{d}t} = \frac{1}{6}\pi d^3(\rho_d - \rho_g)\mathbf{g} + \frac{1}{2}C_D\frac{\pi d^2}{4}\rho_g(\mathbf{u}_g - \mathbf{u}_d)|(\mathbf{u}_g - \mathbf{u}_d| \tag{7}$$

where subscripts d and g refer to droplet and gas, respectively; u is the velocity, and g is the acceleration of gravity, considered parallel to the mean gas velocity. This equation is solved in the two-dimensional system of axial (z) and radial (r) coordinates, to calculate the axial distance covered by the drop once the radial distance is known. The aerodynamic drag coefficient, C_D, can be expressed as (Rowe and Henwood, 1961):

$$C_D = \frac{24}{Re_d}(0.15 + Re_d^{0.687}) \tag{8}$$

where Re_d is the droplet Reynolds number based on particle velocity relative to fluid velocity, and on fluid kinematic viscosity, ν_f. This expression for C_D holds for $Re_d < 200$. In the annular flow regime analyzed in the present study, droplet Reynolds number range from few units up to 200.

To solve eq. (7), the initial velocity vector and the initial position of entrained drops must be specified. To this purpose, the following results presented in by Andreussi and Azzopardi (1983, 1984), can be used.

(1) The direction averaged component of the ejection velocity in the cross-sectional plane, v_i, can be

related to the velocity of the gas phase, u^*, by the equation:

$$v_i = 12.0\,u^*\sqrt{\rho_g/\rho_l}. \tag{9}$$

(2) The direction averaged path covered by droplets in the cross-sectional plane is equal to $0.7D$, D being the pipe diameter. It is worth noting that this value is slightly larger than $2D/\pi$, the length of the average chord, thus suggesting the ejection angle being uniformly distributed (considering a pipe cross section, the ejection angle is formed by the droplet initial direction projected onto the cross section and the tangent to the section at the drop ejection location).

The axial component of droplet initial velocity can be assumed roughly equal to the liquid film velocity at the gas–liquid interface which is typically less than 10% of the gas velocity and, in any case, is of the order of the gas friction velocity. Since this work is focused on the droplet dynamics after the entrainment, ejection mechanics are not considered. Therefore, at the entrainment, the droplet is supposed to be at the wall ($z = 0$, and $r = D/2$) with the following initial velocity components: $u_z = u^*$; $u_r = v_i$.

These initial conditions allow the axial distance, z_d, covered by a generic droplet of diameter d leaving the wall layer and travelling a transverse distance in the cross-sectional plane equal to $0.7D$, to be calculated. From this distance and any given droplet size distribution it is possible to obtain the impact deposition coefficient, k_I, in the following form (Andreussi and Azzopardi, 1983):

$$k_I = \frac{u_g D}{4}\frac{\int_0^\infty F(z)\,dz}{\int_0^\infty F(z)\,z\,dz} \tag{10}$$

where $F(z)$ represents the mass fraction of droplets that are not deposited after a distance z from the location of their entrainment. The ratio between integrals in eq. (10) can be expressed as

$$\frac{\int_0^\infty F(z)\,z\,dz}{\int_0^\infty F(z)\,dz} = C_0\overline{z_d} \tag{11}$$

where $\overline{z_d}$ represents the axial distance covered by the mean size droplet which covers a distance equal to $0.7D$ in the crosstream direction. The coefficient C_0 accounts for all the deviations associated with the averaging procedures adopted. It is expected that C_0 is of order of magnitude equal to one.

In conclusion, the deposition coefficient for direct impaction can be expressed as:

$$k_I = u_g D/4C_0\overline{z_d} \tag{12}$$

with $\overline{z_d}$ obtained through the integration of eq. (7).

3. EFFECT OF COALESCENCE ON DROPLET MOTION

3.1. *Collisions and coalescence: interaction probability*

When a swarm of droplets moves through a turbulent gas stream, interactions are likely to occur. Some interactions lead to stable coalescence between droplets, while others do not. Indeed, due to the presence of particles themselves, flow streamlines are modified and the smaller particle tends to follow the streamlines bending around the larger one. Furthermore, once droplets have effectively collided, they may separate again (often in two, but also in more drops), or even, if the collision is particularly energetic (and the present context may be the case), droplets may shatter as a consequence of the impact (Ashgriz and Poo, 1990).

A number of researchers (Abrahamson, 1975; Williams and Crane, 1983; Zhang and Davis, 1991) studied droplet–droplet interaction and coalescence. However, in annular flow, the high turbulence intensity, the complexity of droplet generation and ejection processes and the variability of conditions under which droplets interact, hamper a rigorous analysis. On the basis of previous works, in the present study a simpler approach will be followed to express the interaction probability.

Before depositing, a droplet experiences a number of interactions with other droplets. The number of interactions is given by the product between the interaction probability per unit length and the distance covered by the droplet before depositing. This distance scales as the pipe diameter, while the interaction probability per unit length, p, is proportional to the product of the collisional cross section of the interacting droplet A_c, by the droplet number concentration, N_d:

$$p = A_c N_d. \tag{13}$$

The collisional cross section is the area swept by a droplet in its motion relative to the others. Supposing droplets spherical in shape, the collisional cross section is given by:

$$A_c = \frac{\pi}{4}(d' + d)^2 \tag{14}$$

where d' and d are the diameters of colliding droplets. Supposing, for the sake of simplicity, all droplets characterized by the same diameter, the number concentration of droplets can be evaluated as:

$$N_d = \frac{6}{\pi d^3}\frac{G_{le}}{G_{gc}} = \frac{6}{\pi d^3}\frac{\alpha_{le}}{\alpha_{gc}}S \tag{15}$$

where S is the slip ratio between gas and droplets, G_{le} is the specific mass flow of entrained droplets, G_{gc} is the specific mass flow of gas, α_{gc} is the void fraction and α_{le} is the liquid entrainment fraction. Since $\alpha_{gc} \simeq 1$, and characterizing droplet size by the Sauter mean diameter, d_{32}, the interaction probability per unit length is

$$p = 6S\alpha_{le}\frac{1}{d_{32}}. \tag{16}$$

In order to characterize droplet–droplet interactions by a dimensionless parameter, the interaction probability, p_i, is defined as the product of the interaction

probability per unit length, p, by the pipe diameter

$$p_i = S\alpha_{le}\frac{D}{d_{32}} \tag{17}$$

where, for simplicity, the numerical coefficient has been dropped. The probability of coalescence. p_c, is obtained as follows:

$$p_c = p_i \varepsilon_c \tag{18}$$

where ε_c is the coalescence efficiency, which is defined as the ratio of the coalescence rate to the collision rate.

3.2. *Effect of coalescence on droplet motion in the cross section*

After ejection from the liquid film, a droplet moves through the gas core before depositing. Other droplets are ejected from other locations and interactions are likely to occur. If the motion of the droplets is projected on a cross section of the pipe, two interacting droplets move along two intersecting chords and their interaction may be studied with a two-dimensional model. The purpose of this model is to assess the influence of droplet–droplet interactions on the total time spent by each droplet in the gas core. This model is applicable to both large and small droplets, regardless of the mechanisms which dominate their motion. Indeed, small droplets fully entrained by the gas core move at about the same axial velocity, and interact because of lateral diffusive motions. For the sake of simplicity, the two interacting droplets are supposed of equal size.

The model is based on the schematics presented in Fig. 1. A drop is ejected from the liquid film with random angle ($0 < \alpha < \pi$) and a given transverse velocity. This droplet does not change its velocity but upon interaction with another droplet. It is assumed that the droplet may interact, at most once, with another droplet which has the same velocity and random transverse direction. The two droplets travel at the same axial velocity. In this part of the study, there is no need to evaluate separately interaction probability and coalescence efficiency: the characteristic variable is the coalescence probability, p_c. After the interaction, the new drop moves along a new direction forming an angle β with the original direction of the first drop, with a doubled mass and velocity proportional to the original one multiplied by the cosine of the angle β (laws of inelastic collision are applied). Any droplet is allowed to interact at most once and the coalescence probability p_c is uniform.

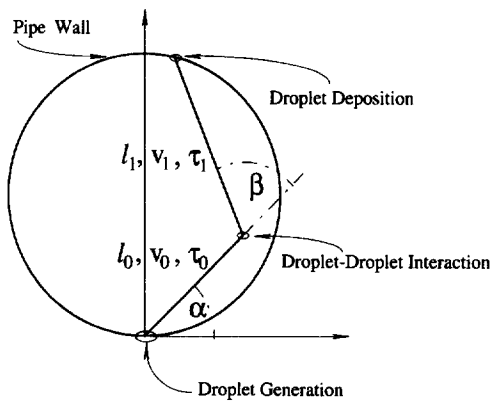

Fig. 1. Reference frame for droplet motion in the cross section.

To get into further detail, let us consider a droplet ejected from the liquid film at an angle α, as presented in Fig. 1 where the main variables are reported. For the sake of simplicity, variables are made dimensionless so as to have a unit pipe diameter and a unit initial velocity modulus. The coalescence probability, p_c, is the probability a droplet has to interact with another droplet and to coalesce with it between the distance l and $l + \mathrm{d}l$. The coalescence probability is assumed uniform along the trajectory of the droplet (it implies just the assumption of uniform droplet concentration in the cross section). Therefore, the probability for the droplet to cover a distance l_0 without interacting with other droplet is $\mathscr{P}_l = p_c \exp[-p_c l]$. This is also the fraction of droplets ejected in the direction α which interact between l and $l + \mathrm{d}l$. Some droplets, however, may cover the whole distance to the wall, which is $\sin\alpha$ (the length of the chord) and deposit without interacting: the fraction of these droplets is $\exp[-p_c \sin\alpha]$. Therefore, the average distance covered before any interaction (either another droplet or the wall) by droplets ejected at an angle α is:

$$l_0(\alpha, p_c) = \int_0^{\sin\alpha} l p_c \exp[-p_c l]\,\mathrm{d}l + \sin\alpha \exp[-p_c \sin\alpha]$$

$$= \frac{1}{p_c} - \frac{1}{p_c}\exp[-p_c \sin\alpha] \tag{19}$$

where it can be seen that $\lim_{p_c \to 0} l_0(\alpha, p_c) = \sin\alpha$.

The ejection angle α has been assumed uniformly distributed in the range $[0, \pi]$. Therefore, the average distance covered by the droplets before any interaction is:

$$\bar{l}_0(p_c) = \frac{1}{\pi}\int_0^{\pi} l_0(\alpha, p_c)\,\mathrm{d}\alpha = \frac{2}{\pi}\int_0^{\pi/2} l_0(\alpha, p_c)\,\mathrm{d}\alpha \tag{20}$$

which is to be integrated numerically.

Since pipe diameter and initial velocity are unitary, the average time spent before the interaction has the same expression and value of the distance covered before the interaction $[\tau(\alpha, p_c) = l_0(\alpha, p_c)$ and $\bar{\tau}(p_c) = \bar{l}_0(p_c)]$.

After the interaction, applying the laws of inelastic collision, the new drop moves away, with a doubled mass, along a new direction forming an angle β with the original direction α. The new direction is the bisectrix of the angle formed by the velocity of the two interacting droplets, and since the direction of the incoming droplet is random, the angle β is uniformly distributed in the range $[-\pi/2, \pi/2]$. The distance covered by the coalesced drops along the new direction from the point where the interaction occurred

and the pipe wall is a function of the initial droplet direction (α), the length covered before the interaction (l_0), the direction under which the coalesced couple of droplets is moving away (β), and the coalescence probability (p_c). It may be expressed as $l_1(\alpha, \beta, l_0, p_c)$, but it is not straightforward to express it as a function of the independent variables. However, it may be observed that l_1 is a random variable, in turn function of random variables independent of each other $(\alpha, \beta, l_0, p_c)$, and it is well known that its average value may be recovered without explicitly deducing its probability distribution. In fact, its average value may be calculated as:

$$\bar{l}_1(p_c) = \int_0^{\pi} \int_{-\pi/2}^{\pi/2} \int_0^{\sin\alpha} l_1(\alpha, \beta, l_0, p_c) \frac{1}{\pi} \frac{1}{\pi} p_c \times \exp[-p_c l_0(\alpha, p_c)] \, d\alpha \, d\beta \, dl_1 \quad (21)$$

where $1/\pi$ is the probability density of the variables α and β (which are uniformly distributed), and $p_c \exp[-p_c l_0(\alpha, p_c)]$ is the probability density of l_0. This equation as well is to be integrated numerically.

After the interaction, the velocity is reduced proportionally to the cosine of angle β, that is $v_1 = v_0 \cos\beta$ and $\tau_1 = l_1/\cos\beta$ (from a momentum balance). Therefore, the average time spent to cover the distance l_1 is:

$$\bar{\tau}_1(p_c) = \frac{1}{\pi} \frac{1}{\pi} \int_0^{\pi} \int_{-\pi/2}^{\pi/2} \int_0^{\sin\alpha} \frac{l_1(\alpha, \beta, l_0, p_c)}{\cos\beta} p_c \times \exp[-p_c l_0(\alpha, p_c)] \, d\alpha \, d\beta \, dl_1. \quad (22)$$

Finally, the total dimensionless path covered by the droplet, l_{tot} is the sum of the path before the collision, l_0, and the path after the collision, l_1. Formally,

$$l_{tot}(\alpha, \beta, l_0, p_c) = l_0(\alpha, p_c) + l_1(\alpha, \beta, l_0, p_c) \quad (23)$$

and its average value is:

$$\bar{l}(p_c) = \bar{l}_0(p_c) + \bar{l}_1(p_c). \quad (24)$$

Analogously, the dimensionless average total residence time τ_{tot} is

$$\overline{\tau_{tot}}(p_c) = \overline{\tau_0}(p_c) + \overline{\tau_1}(p_c) \quad (25)$$

and, explicitly

$$\overline{\tau_{tot}}(p_c) = \frac{1}{\pi} \int_0^{\pi} \left[\int_0^{\sin\alpha} l p_c \exp[-p_c l] \, dl + \sin\alpha \exp[-p_c \sin\alpha] = \frac{1}{p_c} - \frac{1}{p_c} \exp[-p_c \sin\alpha] \right] + \frac{1}{\pi} \frac{1}{\pi} \int_0^{\pi} \int_{-\pi/2}^{\pi/2} \int_0^{\sin\alpha} \frac{l_1(\alpha, \beta, l_0, p_c)}{\cos\beta} p_c \times \exp[-p_c l_0(\alpha, p_c)] \, d\alpha \, d\beta \, dl_1. \quad (26)$$

In Fig. 2 the droplet mean life time before a collision, the mean life time after the collision and the total mean life time are plotted vs the coalescence probability. A remarkable increase of the total life time may be noticed as p_c increases. In Fig. 3 the deposition coefficient for the droplets described by this model, made dimensionless with respect to the value at zero coalescence probability, is plotted vs the coalescence probability. The deposition constant shows a strong dependence upon p_c. Since the deposition coefficient is inversely proportional to the time spent by the droplet in the gas core, in this figure, the dependence of the ratio of the residence time of a droplet in absence of coalescence to the residence time calculated with coalescence effect on the coalescence probability may be observed as well.

The procedure followed in this approach is indeed qualitative, since the model is simplified and cannot hold for higher p_c. Yet it suggests how the collision/coalescence process may appreciably influence the deposition mechanism.

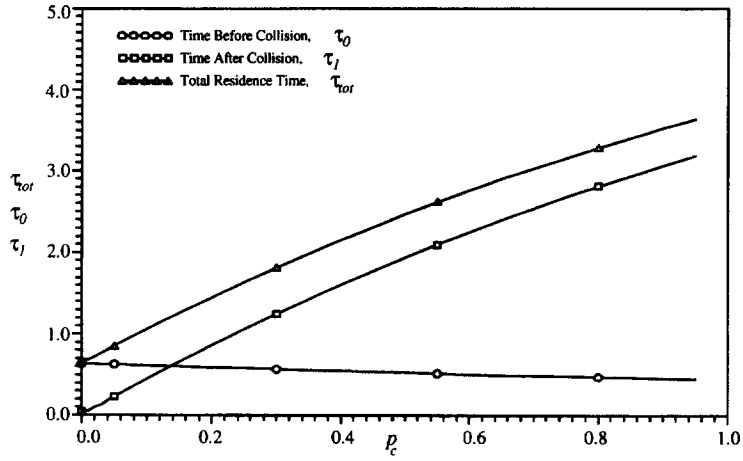

Fig. 2. Effect of coalescence probability on droplet motion in the cross section. Average time before a collision (○), average time after a collision (□) and total residence time (△) vs coalescence probability, p_c, are shown.

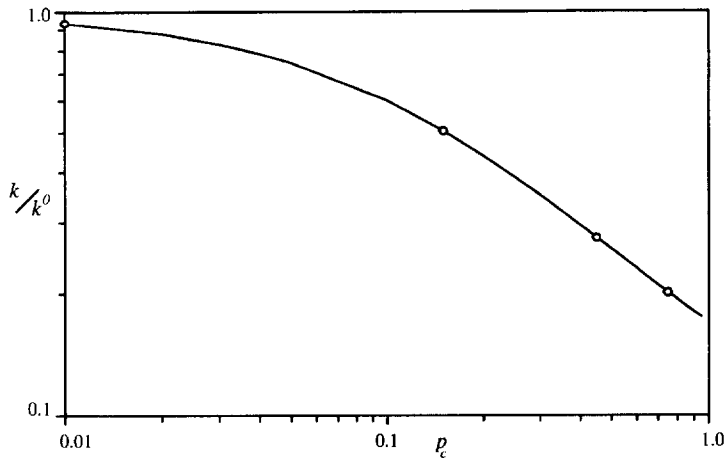

Fig. 3. Effect of interaction probability on droplet deposition coefficient in the cross section. The deposition coefficient, k, divided by the deposition coefficient evaluated at zero coalescence probability, k_0, is plotted vs coalescence probability.

3.3. *Effect of small droplets on the trajectory of a large drop*

Large drops accelerating through the gas core are likely to interact with smaller droplets which are carried by the gas and may catch up with them. The way in which collision and coalescence influence the motion of a large drop may be assessed examining the equation of motion of a single drop. The mass conservation equation for an accelerating spherical droplet of mass m_d, that collides with smaller droplets of mass m' and diameter d' is:

$$\frac{dm_d}{dt} = \dot{n}_c m' \tag{27}$$

where $\dot{n}_c$ is the number of interactions leading to coalescence per unit time due to the sweeping action of the large drop on smaller droplets entrained by the gas:

$$\dot{n}_c = \frac{\pi}{4}(d + d')^2 |\mathbf{u}_g - \mathbf{u}_d| \, \varepsilon_c \frac{G_{le}}{u_g m'}. \tag{28}$$

In this equation, small droplets are assumed to travel at the gas velocity. The momentum balance presented in eq. (7) is modified as follows:

$$\frac{d(m_d \mathbf{u}_d)}{dt} = \frac{1}{6}\pi d_d^3(\rho_l - \rho_g)\mathbf{g} + \frac{1}{2}C_D \frac{\pi d_d^2}{4} \times \rho_g(\mathbf{u}_g - \mathbf{u}_d)|\mathbf{u}_g - \mathbf{u}_d| + \dot{n}_c m' \mathbf{u}_g \tag{29}$$

where the last term represents the contribution given to the drop momentum variation by the interacting small droplets. If the inertial term is expanded and if the diameter of colliding drops d' is assumed negligible compared to the diameter of the target drop, d_d, the momentum equation becomes:

$$\frac{d\mathbf{u}_d}{dt} = \frac{\rho_l - \rho_g}{\rho_l}\mathbf{g} + \frac{3}{4}C_D \frac{\rho_g}{d_d \rho_l}(\mathbf{u}_g - \mathbf{u}_d)|\mathbf{u}_g - \mathbf{u}_d| + \frac{3}{2}\varepsilon_c p_i (\mathbf{u}_g - \mathbf{u}_d)|\mathbf{u}_g - \mathbf{u}_d|. \tag{30}$$

It is interesting to note that, if the drop drag coefficient is assumed constant (Newton's regime), fluid drag and coalescence effect have the same form: that is, the effect of momentum transfer from small droplets may be interpreted as an additional drag on the larger drop which thus accelerates faster in the axial direction. However, to solve a more general and representative case, in this work the drag coefficient shown in eq. (8) was used. The system formed by eqs (27) and (30) was integrated numerically by a fourth-order Runge–Kutta method, in the two-dimensional system of the axial (z) and radial (r) coordinate. The initial conditions were the same used to solve eq. (7) with the additional condition on the initial droplet diameter as explained in the next paragraph.

3.4. *Effect of coalescence on diameter and residence time of large droplets*

As previously described, small droplets fully entrained by the gas catch up with a large drop influencing its motion. The effect is twofold, since the drop experiences both an increased drag (increase of the flight time) and an increase of its mass (increase of diameter). In the paper by Ambrosini *et al.* (1991), the coalescence effect was accounted for to derive a correlation for the droplet Sauter mean diameter. The correlation has the following form:

$$\frac{d_{32}}{h_f} = x_1 \sqrt{\frac{\sigma}{\rho_g f_i u_g^2 h_f}} \left(\frac{\rho_g}{\rho_l}\right)^{x_2} \exp\left[x_3 p_i + \frac{x_4}{We_D}\right] \tag{31}$$

where σ is the liquid surface tension, h_f is the liquid film thickness, f_i is the interfacial friction factor and We_D is the Weber number based on the pipe diameter, $We_D = \rho_g u_g^2 D/\sigma$. The four parameters appearing in eq. (31) have the optimized values: $x_1 = 22.0$, $x_2 = 0.83$, $x_3 = 0.6$ and $x_4 = 99.0$. This correlation, validated against a large set of data [Jepson *et al.*,

(1989) among others], introduces the effect of coalescence through the correction factor $\exp[x_3 p_i]$, which depends on the interaction probability. The coalescence efficiency, not mentioned by Ambrosini *et al.* (1991), may be assumed as included in the dimensionless fitting constant x_3. The increase of droplet mean diameter due to coalescence may be calculated using this correlation.

With the initial diameter, calculated by eq. (31) used without the coalescence contribution, and a value for the coalescence efficiency, ε_c, the system of eqs (27) and (30) may be solved and the diameter increase compared with predictions of eq. (31). In Fig. 4, such comparison is presented as applied to the experimental data obtained by Jepson *et al.* (1989). The best agreement between the present model and the correlation was obtained for a coalescence efficiency equal to 0.16. This value is in agreement with previous considerations and the experimental results relative to the coalescence efficiency (Ashgriz and Poo, 1990; Zhang and Davis, 1991).

The other effect of coalescence is to increase the total drag on the droplet [last term of eq. (30)]. This, in turn, increases the axial distance covered by the droplet, and consequently decreases the value of the impact deposition constant, k_I. In Fig. 5, the effect of coalescence on the impact deposition coefficient may be appreciated. In this figure, the ratio of the deposition constant in presence of coalescence to the one relative to dilute conditions is plotted vs the coalescence probability for different droplet initial diameter. In this computation, the same value of the coalescence efficiency calculated for Fig. 4, $\varepsilon_c = 0.16$, was maintained. As it may be noticed, the effect of coalescence on the deposition coefficient is remarkable. Since the impact deposition coefficient is inversely proportional

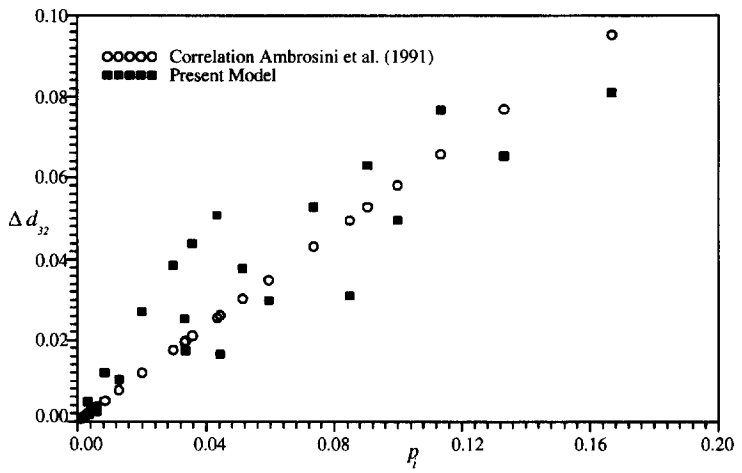

Fig. 4. Evaluation of coalescence efficiency. Comparison of the fractional increase of droplet diameter [$\Delta d = (d - d^{nc})/d$, with $d = d_{32}$, and the superscript *nc* means *no coalescence*] calculated with the present model (with $\varepsilon_c = 0.16$) and with the correlation by Ambrosini *et al.* (1991).

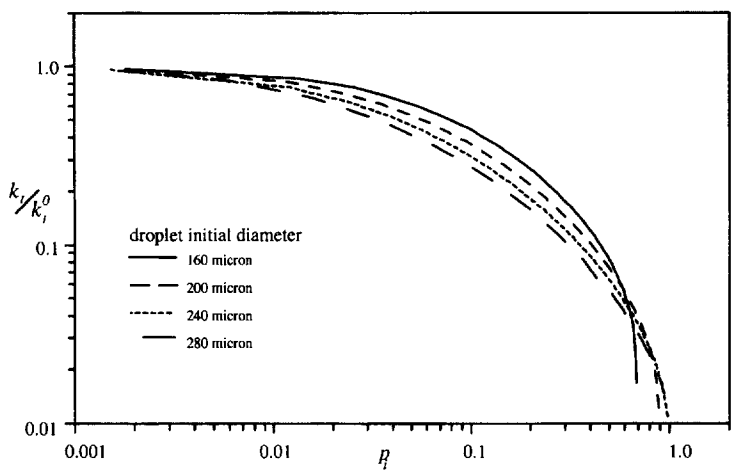

Fig. 5. Effect of interaction probability on droplet impact deposition. The deposition coefficient, k, divided by the deposition coefficient evaluated at zero interaction probability, k_0, is plotted vs the interaction probability. The behavior of droplets of different diameter is presented.

to the axial distance covered by the average drop, $\overline{z_d}$ [see eq. (12)], this figure also represents the ratio of the axial distance calculated in the absence of coalescence to the one calculated accounting for coalescence. Furthermore, from Fig. 5, it is possible to see that droplet motion is strongly affected by the coalescence probability, and is a weaker function of droplet diameter.

4. ANALYSIS OF EXPERIMENTAL DATA

4.1. *Overall deposition coefficient*

In this section, a deposition model which accounts for the effect of coalescence is developed on the basis of previous considerations. The model rests on the basic assumption of the two mechanisms of droplet transfer acting in parallel. This implies that the total deposition rate is given by both contributions of impaction and diffusion deposition. Therefore, the overall coefficient, k, can be calculated as:

$$k = V_I k_I + (1 - V_I) k_D \tag{32}$$

where V_I represents the volume fraction of droplets depositing by impaction, k_I is given by eq. (12), with $\overline{z_d}$ computed by means of eqs (27) and (30) and k_D is evaluated by the equation

$$\widetilde{k_D} = \widetilde{k_D^0} \frac{1}{1 + C_1 p_i}. \tag{33}$$

This correlation is similar to the one proposed by Andreussi (1983) [see eq. (6)], except that coalescence is assumed to depend on the interaction probability rather than on droplet concentration. The coefficient C_1 is an adjustable parameter.

The cumulative volume distribution of droplet size can be evaluated by the equation proposed by Andreussi and Azzopardi (1983), which is based on the Rosin–Rammler distribution, and the fraction V_I is given by

$$V_I = \exp\left[-\left(\frac{1}{2} \frac{d_c}{d_{32}} \right)^2 \right] \tag{34}$$

where d_c is the critical drop diameter at the transition between the two transfer mechanisms, and d_{32} is the Sauter mean diameter calculated adopting the correlation proposed by Ambrosini *et al.* (1991). The diameter to be used in eqs (27) and (30), which will be called d_I, is the volume median diameter of the fraction of droplets with diameter larger than d_c. The critical drop diameter at the transition may be estimated as proposed by Andreussi and Azzopardi (1983). These authors suggested that the ratio between the droplet initial transverse momentum (M_d) and the drag force exerted by turbulent eddies (drag force × eddy characteristic time, $f_d \times T_e$). The eddy characteristic time may be assumed to scale with the ratio between the eddy characteristic length, which in turn scales as the pipe diameter and the friction velocity. Then, this ratio may be expressed as:

$$\frac{M_d}{f_d T_e} \propto \frac{\rho_l v_l d_c}{C_D \rho_g u^* D} = G. \tag{35}$$

The dimensionless group G may be used to determine the transition between random walk and inertially dominated motion. Using the numerical simulations by James *et al.* (1980), Andreussi and Azzopardi (1983) found the transition accurring at $G \simeq 0.7$.

4.2. *Prediction of the deposition coefficient*

The objective of the deposition model is to supply a reliable prediction of the deposition coefficient k from the knowledge of liquid flow rate, gas flow rate and entrained liquid flow rate, which are reported in a number of works [Andreussi (1983), Leman (1985), Jepson *et al.* (1989) and Schadel *et al.* (1980) among others]. The model is based on the use of eq. (32), for the application of which the fraction of inertially moving droplets, and the impact deposition and diffusion coefficients have to be determined. Use of eqs (31), (35) and (34) allows for the determination of d_{32}, d_c and V_I; the interaction probability is determined from eq. (15) knowing d_{32} and the flow rates of entrained liquid and gas core. The diffusion deposition coefficient, k_D, is determined with eq. (33). The calculation of the impact deposition coefficient, requires the use of eqs (27) and (30) to determine the deposition length, $\overline{z_d}$, and the use eq. (12) to determine k_I.

As it is, the model relies on five parameters: C_0, and C_1, which are tunable with a certain degree of freedom, and G, ε_c and $\widetilde{k_D^0}$ which have to be chosen respecting previous literature results.

In this section, eq. (32) is applied to available experimental data, and data by Andreussi (1983) are the most suitable to be compared with the model since they were obtained under conditions for which both deposition mechanisms were important. These data are relative to air–water downward flow in a vertical 0.024 m diameter pipe, and deposition rates were measured by the steady film tracer method (Quandt, 1965). This method is based on the injection of a dye (or salt solution) into the liquid film. The liquid film flow rate is determined from measurements of the tracer concentration at different location downstream and from the initial tracer concentration determined by extrapolation of measurements. The initial decrease of the dye concentration is used to determine the deposition rates. Therefore, the determination of deposition rates, and in turn of the deposition coefficient, is based on indirect measurements.

The deposition constant, made dimensionless by the gas friction velocity, was calculated and plotted along with the experimental values in Fig. 6, as a function of the interaction probability. As can be seen, the model slightly underpredicts the experimental data in the region of intermediate values of the interaction probability, but, in general, the agreement is good. The optimized values for the two parameters C_0, and C_1, are respectively 3.5 and 5.5. The other constants present in the model have been used with the values $\widetilde{k_D^0} = 0.13$, $G = 0.9$ and $\varepsilon_c = 0.20$, which optimize the fit of the model and respect previous results.

In Fig. 7(a) and (b), the dimensional deposition coefficients obtained by Andreussi (1983) and the

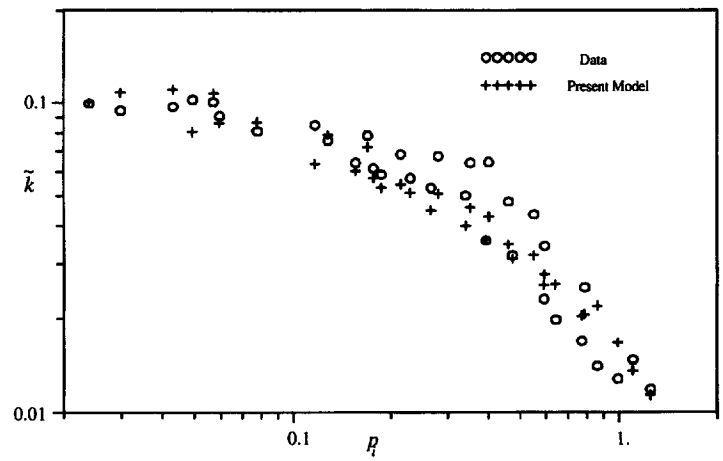

Fig. 6. Application of the deposition model to data by Andreussi (1983). Dimensionless deposition constant vs the interaction probability.

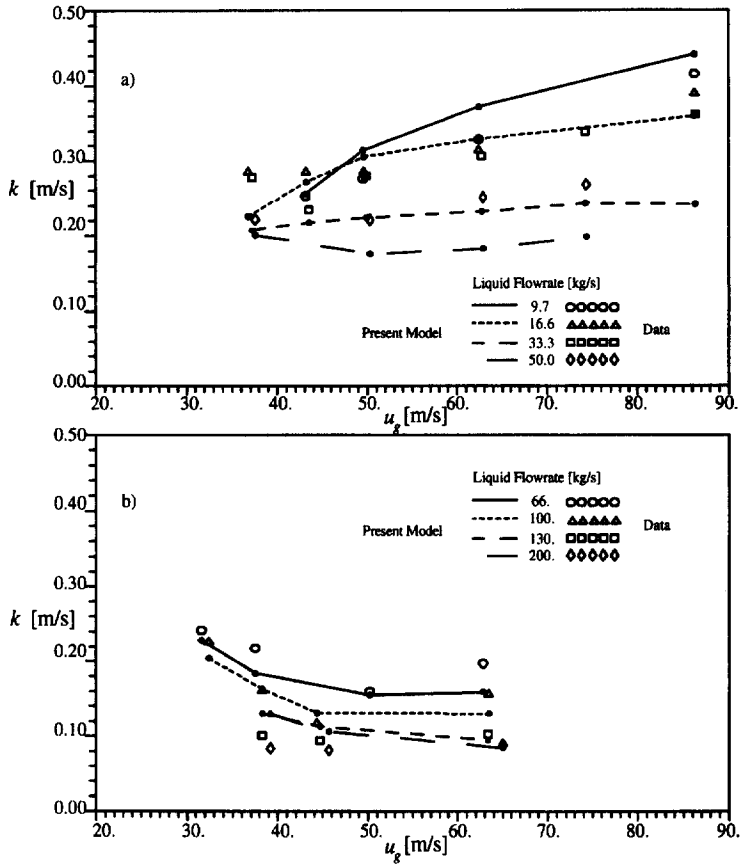

Fig. 7. Application of the deposition model to data by Andreussi (1983). Dimensional deposition constant at different gas velocities. Open symbols represent data; lines connect calculated results (solid symbols). (a) Low liquid flow rates; (b) high liquid flow rates.

calculated ones are plotted as a function of the actual gas velocity for different values of the total liquid flow rate. In these figures, the symbols represent experimental data and the lines connect calculated points for ease of comparison.

The trend of k at different liquid flow rates allows some observations to be made. Basically, the effect of an increase of the liquid flow rate results in a reduction of the deposition coefficient because of the effect of coalescence on both deposition mechanisms. An increase of the gas velocity reduces the average droplet size and increases the turbulent diffusion, thus giving more relevance to the diffusive transport mechanism. At larger liquid flow rates, the deposition

coefficient seems fairly independent of the gas velocity. At low liquid flow rates k increases with the gas velocity, since the velocity increase leads to an enhanced turbulent diffusivity. At intermediate liquid flow rates, the deposition coefficient has a minimum for values of the velocity of about 40.0 m s^{-1}. At lower gas velocities, the impact deposition has a greater importance. As soon as the increase in gas velocity leads to a corresponding decrease in droplet diameter, the droplet initial momentum becomes smaller, droplets do not deposit with a free flight mechanism and the transfer of a larger fraction of droplets is dominated by the diffusive mechanism.

The application of the model to these data is encouraging. In fact, the influence of both gas velocity and liquid flow rate on the relative importance of the two deposition mechanisms seems to be well captured.

5. DISCUSSION AND CONCLUSIONS

In gas–liquid annular flow, the transfer of droplet from the gas core to the liquid film is controlled by two different mechanisms: deposition by turbulent diffusion and by direct impaction. The diffusion mechanism controls the deposition of droplets small enough to be fully entrained by the gas. The impact mechanism (free flight through the gas core) controls the transfer of droplets with initial momentum large enough to keep their trajectory relatively unaffected by the turbulent components of the gas velocity. At large droplet concentration, both deposition mechanisms appear to be affected by droplet–droplet interactions.

In this work, the effect of coalescence on droplet motion has been theoretically assessed and a deposition model which accounts for the contribution of the two deposition mechanisms and the effect of coalescence has been developed and assessed against experimental data.

The effect of collisions and coalescence on the motion of a large drop was studied considering the case of a drop which interacts with smaller, fully entrained droplets (axial interaction), and the case of two equally sized drops, which move along intersecting chords in the cross section (lateral interaction). The solutions of these two cases allowed us to verify that coalescence plays an important role in lengthening the residence time of a drop in the gas core. This results in a decrease of the deposition constant and allows a simple physical explanation of the experimental observations. Furthermore, this model explains the effects of droplet concentration on droplet size, detected by Azzopardi *et al.* (1979) and by Ambrosini *et al.* (1991).

On the basis of these results, a deposition model has been developed. The contribution of the two deposition mechanisms was distinguished identifying two deposition coefficients, by diffusion and by impaction. The relative weight of the two coefficients was determined by the volume fraction of droplets which followed diffusion or impaction mechanisms, respectively. The calculated deposition coefficients have been compared against experimental data and a good agreement has been found.

Acknowledgments—Financial support from CEC, JOULE2 Programme, under Grant No. *JOU2-CT-92-0108* and from the Italian Ministry of University and Scientific and Technological Research is gratefully acknowledged.

NOTATION

A_c collisional cross section of two colliding drops, m^2
C_D aerodynamic drag coefficient, m s^{-1}
C_E droplet concentration, kg m^{-3}
C_0 constant in eq. (11)
C_1 constant in eq. (33)
d, d_d droplet diameter, m
d_c droplet diameter at the transition, m
d_I mean diameter of impact depositing droplets, m
d_{32} droplet Sauter mean diameter, m
D pipe diameter, m
f_i friction factor
g gravity acceleration, m s^{-2}
G_{gc} specific mass flow of gas, kg m^{-2} s^{-1}
G_{le} specific mass flow of entrained liquid, kg m^{-2} s^{-1}
h_f film thickness, m
k deposition coefficient, m s^{-1}
k_D diffusional deposition coefficient, m s^{-1}
k_I impact deposition coefficient, m s^{-1}
l dimensionless total path in the cross section
l_l Lagrangian microscale of turbulence, m
l_0 dimensionless path before collision in the cross section
l_1 dimensionless path after collision in the corner section
L_e turbulent eddy characteristic length, m
m_d droplet mass, kg
M_d droplet initial transverse momentum, kg m s^{-2}
$\dot{n}_c$ number of interactions leading to coalescence per unit time, s^{-1}
N_d number concentration of droplets, m^{-3}
p interaction probability per unit length, m^{-1}
p_c interaction probability
p_c coalescence probability
R_D deposition rate, kg m^{-2} s^{-1}
Re_d droplet Reynolds number
S slip factor
S_t stokes number
t time, s
T_e turbulent eddy characteristic time, s
u velocity, m s^{-1}
u_d droplet velocity, m s^{-1}
u_g gas velocity, m s^{-1}
u^* shear velocity, m s^{-1}
u' velocity fluctuations, m s^{-1}
v_i droplet ejection velocity, m s^{-1}
We_D droplet Weber number

Greek letters
α ejection angle

β angle after a collision
α_{gc} volume fraction of gas
α_{le} volume fraction of entrained liquid
ε_c coalescence efficiency
ε_d droplet diffusivity, $m^2\ s^{-1}$
ε_f fluid diffusivity, $m^2\ s^{-1}$
μ_f fluid viscosity, $kg\ m^{-1}\ s^{-1}$
ν_f fluid kinematic viscosity, $m^2\ s^{-1}$
ρ_g gas density, $kg\ m^{-3}$
ρ_l liquid density, $kg\ m^{-3}$
σ surface tension, $kg\ m^{-1}\ s^{-2}$
τ dimensionless total time spent in the cross section
τ_0 dimensionless time before collision in the cross section
τ_1 dimensionless time after collision in the cross section
τ_i interfacial shear stress, $m\ s^{-1}$
τ_d droplet relaxation time, s
τ_f fluid characteristic time scale, s
τ_{lf} Lagrangian fluid characteristic time scale, s

Superscripts

^{0} no coalescence effect
$\sim$ dimensionless (for the deposition coefficient)
$\bar{}$ average

REFERENCES

Abrahamson, J., 1975, Collision rates of small particles in a vigorously turbulent fluid. *Chem. Engng Sci.* **30**, 1371–1379.

Ambrosini, W., Andreussi, P. and Azzopardi, B. J., 1991, A physically based correlation for drop size in annular flow. *Int. J. Multiphase Flow* **17**, 497–507.

Andreussi, P., 1983, Droplet transfer in two-phase annular flow. *Int. J. Multiphase Flow* **9**, 697–713.

Andreussi, P. and Azzopardi, B. J., 1983, Droplet deposition and interchange in annular two-phase flow. *Int. J. Multiphase Flow* **9**, 681–695.

Andreussi, P. and Azzopardi, B. J., 1984, On the entrainment of drops by the gas in two-phase annular flow. *Chem. Engng Sci.* **39**, 1426–1428.

Ashgriz, N. and Poo, J. Y., 1990, Coalescence and separation in binary collision of liquid drops. *J. Fluid Mech.* **221**, 183–204.

Azzopardi, B. J., Freeman, G. and King, D. J., 1980, Drop sizes and deposition in annular two phase flow. UKAEA Report, AERE-R 9634.

Cousins, L. B. and Hewitt, C. F., 1968, Liquid phase mass transfer in annular two-phase flow. UKAEA Report, AERE-R 5657.

James, P. W., Hewitt, C. F. and Whalley, P. B., 1980, Droplet motion in two-phase flow. UKAEA Report, AERE-R 9711.

Jepson, D. M., Azzopardi, B. J. and Whalley, P. B., 1989, The effect of gas properties on drops in annular flow. *Int. J. Multiphase Flow* **15**, 327–339.

Lee, M. M., Adrian, R. J. and Hanratty, T. J., 1989, The intepretation of droplet deposition measurements with a diffusion model. *Int. J. Multiphase Flow* **15**, 459–469.

Leman, G. W., 1985, Atomization and deposition in two-phase annular flow: measurement and modeling. Ph.D. dissertation, University of Illinois at Urbana-Champaign, Urbana, IL, U.S.A.

Leman, G. W., Agostini, M. and Andreussi, P., 1985, Tracer analysis of developing two-phase annular flow. *PysicoChem. Hydrodyn.* **6**, 223–237.

McCoy, D. D. and Hanratty, T. J., 1977, Rate of deposition of droplets in annular two-phase flow. *Int. J. Multiphase Flow* **3**, 319–331.

Namie, S. and Ueda, T., 1972, Droplet transfer in two-phase annular mist flow (Part1, Experiment of droplet transfer rate and distribution of droplet concentration and velocity). *Bull. JSME* **15**, 1568–1580.

Quandt, E. R., 1965, Measurement of some basic parameters in two-phase annular flow. *A.I.Ch.E. J.* **11**, 311–318.

Rowe, P. N. and Henwood, G. A., 1961, Drag forces in hydraulic model of a fluidised bed—Part I. *Trans. Instn Chem. Engrs* **39**, 43–54.

Schadel, S. A., Leman, G. W., Binder, J. L. and Hanratty, T. J., 1990, Rates and atomization and deposition in vertical annular flow. *Int. J. Multiphase Flow* **16**, 363–374.

Williams, J. J. and Crane, R. I., 1983, Particle collision rate in turbulent flow. *Int. J. Multiphase Flow* **9**, 421–435.

Young, J. B. and Hanratty, T. J., 1991, Optical studies on the turbulent motion of solid particles in a pipe flow. *J. Fluid Mech.* **231**, 665–668.

Zhang, X. and Davis, R. H., 1991, The rate of collisions due to Brownian or gravitational motion of small drops. *J. Fluid Mech.* **230**, 479–504.